

G. Tardini, J. Ferreira, P. Mantica, A.G. Peeters, T. Tala, K.D. Zastrow, M. Brix,
C. Giroud, G.V. Pereverzev and JET EFDA contributors

Angular Momentum Studies with NBI Modulation in JET

"This document is intended for publication in the open literature. It is made available on the understanding that it may not be further circulated and extracts or references may not be published prior to publication of the original when applicable, or without the consent of the Publications Officer, EFDA, Culham Science Centre, Abingdon, Oxon, OX14 3DB, UK."

"Enquiries about Copyright and reproduction should be addressed to the Publications Officer, EFDA, Culham Science Centre, Abingdon, Oxon, OX14 3DB, UK."

Angular Momentum Studies with NBI Modulation in JET

G. Tardini¹, J. Ferreira², P. Mantica³, A.G. Peeters⁴, T. Tala⁵, K.D. Zastrow⁶,
M. Brix⁶, C. Giroud⁶, G.V. Pereverzev¹ and JET EFDA contributors*

JET-EFDA, Culham Science Centre, OX14 3DB, Abingdon, UK

JET-EFDA, Culham Science Centre, Abingdon, OX14 3DB, United Kingdom

¹*Max-Planck-Institut für Plasmaphysik, EURATOM/MPI Association, Boltzmannstrasse 2,
D-85748 Garching, Germany*

²*Associação EURATOM/IST, Instituto de Plasmas e Fusão Nuclear, Instituto Superior Técnico,
Av Rovisco Pais, 1049-001 Lisbon, Portugal,*

³*Istituto di Fisica del Plasma, EURATOM/ENEA-CNR Association, 20125, Milano, Italy*

⁴*Centre for Fusion, Space and Astrophysics, University of Warwick, UK*

⁵*Association EURATOM-Tekes, VTT, P.O. Box 1000, FIN-02044 VTT, Finland*

⁶*EURATOM-UKAEA Fusion Association, Culham Science Centre, OX14 3DB, Abingdon, OXON, UK*

** See annex of F. Romanelli et al, "Overview of JET Results",
(Proc. 22nd IAEA Fusion Energy Conference, Geneva, Switzerland (2008)).*

ABSTRACT

In the present work we apply the neutral beam modulation technique to a set of JET discharges in order to obtain information on the radial transport of the toroidal angular momentum. This perturbative technique has been often used for heat transport in the past; it is particularly suited to separate possible pinch terms from the momentum diffusivity, otherwise impossible to decouple with a steady-state momentum balance analysis alone. In this paper a model based on the Ion Temperature Gradient (ITG) turbulence, which consists of a constant Prandtl number of the order unity combined with an inward pinch, is validated against data from the JET experiment. The machine size and the good space and time resolution of the Charge Exchange system make JET particularly suitable for this study. Sensitivity studies assess the accuracy range of our predictive modelling.

INTRODUCTION

A finite toroidal angular velocity is widely believed to reduce ion heat transport in tokamaks through its radial derivative, leading to a partial or even a complete suppression of the Ion Temperature Gradient (ITG) driven mode, as predicted by theory [1] [2][3] and observed for instance in ion internal transport barriers [4][5][6].

Intrinsic rotation has been observed in several tokamaks [7][8][9][10][11][12], and a sizeable toroidal velocity in ITER is not excluded despite the expected low torque density. Intrinsic rotation can be explained either by some source terms neglected so far, or by a convective inward pinch, transferring momentum from the plasma edge to the center, or by an off-diagonal transport coefficient, independent of the toroidal velocity itself, related for instance to the pressure gradient. However, a momentum balance analysis based on the steady-state profiles alone cannot distinguish between diffusive and convective contributions, since it allows to determine only an effective viscosity $\chi_{\phi}^{eff} = \Gamma_{\phi}/(n_i m_i \nabla \varphi)$, where Γ_{ϕ} is the toroidal angular momentum flux, n_i the ion density and m_i the ion mass. In this work a perturbative technique is used, in order to decouple convection and diffusion and provide an estimate of a possible pinch velocity. The Neutral Beam Injection (NBI) power is modulated at 6.25 Hz in order to produce a periodic perturbation of the torque density. The time resolved measurement of the angular velocity profiles allows to observe the plasma response.

The ITG mode is regarded as the physics mechanism dominating ion heat transport in tokamaks' H-mode plasmas [13] [14]. According to ITG based theories [15], the ratio of plasma momentum and ion heat diffusivity, called Prandtl number, is approximately constant and of order one. The validity of this theoretical result has been investigated in several machines [16][17], delivering a range of Prandtl numbers for the different machines and for different experimental conditions. One of the aims of this paper is to study the validity of the assumption of a constant Prandtl number with simultaneous steady-state and perturbative analysis, thus providing a constraining test for the

model.

Recent developments of the gyrokinetic theory predict the existence of a momentum pinch in a rotating plasma [18]. Such a pinch term is predicted to be non-negligible in tokamaks in a range of relevant experimental conditions. The approximate formula for ITG dominated plasmas derived in reference [18] is used in this work. The existence of a momentum pinch could partly explain the discrepancy between Prandtl numbers in different machines [17], thereby increasing the physics understanding of toroidal momentum transport.

The paper is structured as follows: in Section the JET experiments are presented, as well as the plasma parameters used and the beam setup. Section contains the experimental analysis of the perturbed profiles, including the time-dependent reconstruction of the different torque terms. In Section , the measured profiles are predicted with a simplified model based on a constant and uniform Prandtl number. Finally, conclusions are drawn.

EXPERIMENTAL SETUP

There are mainly three mechanisms for the momentum transfer from beam fast ions to the thermal plasma: via collisions, $\mathbf{J} \times \mathbf{B}$ and thermalisation [19]. The collisional torque is the resulting momentum exchange of single Coulomb scattering processes between beam and thermal ions. The $\mathbf{J} \times \mathbf{B}$ term is a consequence of the radial current generated by the displacement of a trapped fast ion from its birth location to the average position of its banana orbit. Therefore, the $\mathbf{J} \times \mathbf{B}$ torque is applied on the time scale of a banana orbit, which is much faster than the collisional momentum transfer taking place on a beam slowing down time scale [20]. The thermalisation torque consists of the momentum carried by the slowed down beam ions when they start to be considered thermal. Its magnitude depends, of course, on the energy threshold defining a thermal ion; in most cases its contribution is, however, negligible, as shown in Section .

The $\mathbf{J} \times \mathbf{B}$ torque has the advantage of being spatially localised in the region around half radius, as a compromise between the beam deposition and the maximum density of trapped ion orbits [20]. The radial localisation of the perturbed torque is, of course, favourable for the experimental analysis of angular momentum transport. The time scale of the $\mathbf{J} \times \mathbf{B}$ torque is instantaneous compared to the beam slowing down time and the angular momentum confinement time. A short modulation period makes the $\mathbf{J} \times \mathbf{B}$ contribution dominant at the fundamental modulation frequency. Reducing the perturbative collisional torque is beneficial also to obtain a clearer phasing of the torque, since the collisional term has a significant time delay. The momentum diffusivity is believed to be linked to ion heat transport [16], while the latter is known to increase with additional ion heating power in ITG dominated plasmas [21][13][14]. Therefore, a modulation period shorter than the beam slowing down time is expected to reduce the diffusivity perturbation, which is desirable since the torque density is modulated as well. Fast modulation has also the advantage of reducing the induced periodic plasma displacement due to the perturbation of the total plasma pressure and, consequently, of the Shafranov shift. Such a space modulation introduces a spurious periodic signal in the charge

exchange measurements if the background angular velocity has a finite gradient.

The time resolution of the Charge eXchange diagnostics, which we set to 10 ms, is not a strong limitation to a fast modulation frequency. The dominant constraint turns out to be the hardware lower limit for the off phase of the neutral beams, as long as 60 ms. To have a reliably periodic waveform we set the off phase to 80 ms, which at 50 % duty cycle means a modulation period of 160 ms. This is larger by almost a factor of 2 than the beam slowing down time calculated by TRANSP for the discharge #66128.

In addition, ICRH power is applied with the aim to enhance the overall transport level without adding any strong torque. Lower Hybrid pre-heating is applied in the early phase of the discharges in order to keep the minimum q high and hence avoid sawtooth activity, which would make the analysis less accurate.

A reliable waveform with many identical periods and constant background plasma parameters is important to maximise the signal to noise ratio of the perturbative signal. Unfortunately, several discharges did not feature the wished reliability of the waveform, as several periods were corrupted or a modulated PINI failed. This reduces the set of discharges available for transport analysis and for the predictive modelling. In Fig. 2 (a) we show the time traces of the NBI heating power in a succesful strong modulation case, namely discharge #66128. We chose the time interval with the best compromise between stable background T_i , ω_ϕ profiles and regular P_{NBI} modulation. For discharge # 66128 it is the time interval between 10.44 and 13 s, as shown in Fig. 2. In Fig. 2 (c) and (d) the time traces of T_i and ω_ϕ show that both signals are significantly modulated. Unfortunately, the Thomson scattering density profile is missing for discharge # 66128. Given the similarity with the #66130 discharge, except for a less reliable PINIs waveform in the latter discharge, the density profile shape is assumed to be the same. The density profile for the discharge #66128 is normalised with the ratio of the respective interferometry measurements.

MOMENTUM TRANSPORT ANALYSIS

Interpretive runs of the TRANSP code have been performed, in particular using its Monte Carlo package NUBEAM [22] for the time-dependent reconstruction of the NBI particle, heat and torque deposition profiles. The code allows to separate the different torque contributions, in particular the $\mathbf{J} \times \mathbf{B}$ and the collisional torque densities. In this way it is possible to determine to which extent the experimental goals, in particular the radial localisation, are achieved. Fig. 3 shows the average torque profile of #66128, a strong modulation discharge. The $\mathbf{J} \times \mathbf{B}$ term is indeed roughly localised at half radius. Its contribution is significant, but not dominant. The perturbed torque density profile for a given frequency, however, is different. Fig. 4 shows the amplitude (a) and phase (b) of the Fourier transform of the different torque density terms at the fundamental modulation frequency. The phase is relative to the NBI power modulation phase. The modulated torque density profile at the fundamental frequency can be seen to be more strongly determined by the $\mathbf{j} \times \mathbf{b}$ torque, as expected. The localisation, however, is far from satisfactory and there is essentially no source free

region in the radial domain. The magnitude of the modulated torque, on the other hand, is large enough to generate a sizeable modulation of the toroidal angular velocity, as shown in Fig. 5, thus allowing for the analysis of the transport coefficients. The first channel of the charge exchange diagnostics is measuring on the high field side. The phase jump will be discussed in detail in section .

MOMENTUM TRANSPORT EMPIRICAL MODELLING

The predictive simulations are performed by means of the flexible ASTRA code [23]. The code allows an arbitrary boundary condition for the toroidal angular momentum transport equation. We choose it to be the experimental value of the angular velocity at $\rho_{tor} = 0.8$, where ρ_{tor} is the normalised square root of the toroidal flux. The momentum diffusivity can be input as a formula with any plasma parameters dependence. In particular it can be chosen to be proportional to the time-dependent ion heat diffusivity derived from the experimental T_i profile. Any form of pinch velocity can be implemented as well. Finally, arbitrary transport equations can be solved, in particular the momentum transport equations with both definitions of the momentum diffusivity χ_ϕ and χ_L (see Section) are solved simultaneously. The reconstruction of the NBI particle, heat and momentum sources is done with the TRANSP code, which contains the accurate Monte Carlo package NUBEAM to simulate the injection and orbit of the suprathermal beam ions [22]. The equilibrium is solved with ASTRA's internal ESC equilibrium solver [24], which allows to take the time-dependent experimental shape of the last closed flux surface as boundary condition.

A simple assumption is made concerning the radial momentum diffusivity profile, which is taken to be proportional to the ion heat diffusivity, the ratio (Prandtl number) being kept constant in time and space. More theory based models exist [25] [26] but they have not yet been systematically validated against present day steady-state discharges, so it is premature to test them on transient experiments. The assumption of a constant Prandtl number is based on the ITG mode physics but is, of course, simplified, relying in particular on adiabatic electrons. A realistic dependence of the Prandtl number on the plasma parameters for ITG turbulence retaining the effect of kinetic electrons is discussed in [27].

The χ_i was determined from the ion power balance analysis; since both the ion heat source and T_i are modulated in the experiments discussed here, χ_i is time-dependent. Within $\rho_{tor} = 0.2$ the ion heat effective diffusivity has large uncertainties, due to the lesser accuracy of the charge exchange measurements in the plasma center and to the low T_i gradients and ion heat sources. Therefore, the assumed diffusivity is also expected to be rather unaccurate in the very central region of the plasma. Moreover, the assumption of a constant Prandtl number is based on ITG physics, which plays no major role inside $\rho_{tor} = 0.2$ nor outside $\rho_{tor} = 0.8$.

Recently a pinch velocity due to Coriolis-like drifts in a rotating plasma has been derived [18]. This term is included in the modelling according to the following simplified formula, fitting the

gyrokinetic simulations of a density gradient scan presented in [18]:

$$\frac{Rv_{CP}}{\chi_\phi} = -2.1 - 0.37 \frac{R}{L_{n_e}} \quad (1)$$

where R is the tokamak major radius, v_{CP} is the Coriolis pinch term and $L_f = |f/\nabla f|$ is the gradient length of any profile f . Negative velocity v_{CP} corresponds to an inward pinch.

DEFINITION OF THE TOROIDAL MOMENTUM DIFFUSIVITY

Some care is required as for the definition of χ_ϕ in the toroidal angular momentum transport equation. In the literature, two definitions are used, reflecting two slightly different physical approaches. For clarity, we call them χ_ϕ and χ_L according to the following definitions:

$$\frac{\partial M}{\partial t} = T + \frac{\partial}{\partial V} \left[\frac{\partial \rho}{\partial V} n_i m_i \chi_\phi < R^2 (\nabla \rho^2)^2 > \frac{\partial \omega_\phi}{\partial \rho} \right] \quad (2)$$

$$\frac{\partial M}{\partial t} = T + \frac{\partial}{\partial V} \left[\frac{\partial \rho}{\partial V} \chi_L < R^2 (\nabla \rho^2)^2 > \frac{\partial (n_i m_i \omega_\phi)}{\partial \rho} \right] \quad (3)$$

χ_L is related more directly to the conservation of the total toroidal angular momentum, whereas χ_ϕ is more consistent with the usual definitions of the electron and ion heat effective diffusivities χ_e and χ_i . Both definitions are valid, but they differ in case of peaked density profile. Neglecting ∇Z_{eff} it is:

$$\chi_\phi = \chi_L \left(1 + \frac{L_{\omega_\phi}}{L_{n_e}} \right) \quad (4)$$

Since typically $L_{\omega_\phi} \approx 0.5 * L_{n_e}$ in JET H-mode plasmas, χ_ϕ is larger than χ_L by some 30 %. This is not enough to explain the strong variation of the Prandtl number observed in different tokamaks [17], but still it introduces a significant difference in the value of the Prandtl number itself. We call $\text{Pr}_\phi = \chi_\phi/\chi_i$ and $\text{Pr}_L = \chi_L/\chi_i$ in the following. The effect on the modelling of the JET discharge # 66128 is shown in Fig. 6 and Fig. 7, using $\text{Pr}_\phi=1$ and $\text{Pr}_L=1$, respectively. As the comparison shows, the phase is predicted with similar accuracy, but the amplitude and steady-state profiles are larger choosing χ_L instead of χ_ϕ . Figures 6 and 7 show that the assumption of $\text{Pr}_L=1$ yields indeed flatter profiles than the case $\text{Pr}_\phi=1$. The Coriolis pinch is then switched off to obtain an estimate of its significance under realistic experimental conditions. The prediction of the steady-state and amplitude profiles becomes poorer (dashed line), because the modelled profiles are flatter than the measured ones. The phase profiles are, instead, almost unaffected, as expected. Selecting $\text{Pr}_\phi = 1.5$, the predicted profiles are flatter than the measured ones, as Fig. 8 shows. This improves the agreement with the experimental phase profile, while again the amplitude and steady-state profiles are in agreement with the experiment only if the pinch term is included. Comparing Fig. 8 with Fig. 6 one can estimate the sensitivity of the predictions to the change in transport, which is not straightforward because the source is not localised. In fact, even increasing χ_ϕ by 50 % the modelled amplitude and steady-state profiles do not change significantly, whereas the phase gets indeed flatter and thus closer to the measured profile. The prediction with $\text{Pr}_\phi=0.5$ is shown in Fig.

9. This value of the momentum diffusivity is too low if we add the Coriolis pinch velocity. Without pinch, instead, this is the best choice of the Prandtl number to predict the steady state profile, in fact quite similar to the prediction with $Pr_\phi=1.5$ with pinch term included (see Fig. 8). This is a useful reference, because it is the estimate of the effective Prandtl number considered usually in the steady state analysis, in absence of predictive modelling. It also provides a measure of the difference in Prandtl number due to the Coriolis pinch: in this case, a factor 3. This is of the same order as the oscillation observed comparing different tokamaks and different experiments [17] and is therefore non negligible in such comparative investigations.

The experimental effective χ_i is, in principle, modulated in time, because according to the ITG theory and to experimal observations the ion heat transport increases with additional heating power [21] [13]. Therefore, the time dependence is retained in our modelling, unless stated differently. Taking a χ_i profile averaged over the considered time interval, and keeping it constant in time, improves slightly the matching of the experimental phase profile around mid radius, as shown in Fig. 10. The amplitude and the steady-state profiles are, instead, unaffected.

PERIODIC PLASMA DISPLACEMENT

The equilibria are reconstructed with constraints from the experimental MSE measurements (EFTM equilibrium). A rougher EFIT reconstruction is available as well for comparison. The periodic shift of the boundary surface, together with the time-dependent Shafranov shift induced by the power modulation, gives rise to an additional apparent modulation of the profiles as seen by the charge exchange diagnostics, which measure at fixed points in space. Fig. 11 shows the oscillation of the magnetic axis position, its major radius R_{mag} (a) and the vertical coordinate z_{mag} (b). The TRANSP calculation uses an independent equilibrium solver, taking the last closed surface from the EFTM equilibrium reconstruction. As a consequence, the magnetic axis oscillation is in good agreement with the EFTM values than with the EFIT reconstruction, which features stronger oscillation amplitude for R_{mag} (Fig. 11), possibly due to the reduced time resolution of 30 ms, compared to 10 ms for the MSE-unconstrained EFIT. The ASTRA code allows input profiles to be functions of $\{R, z\}$, mapping them into different coordinates according to ASTRA's evolving equilibrium reconstruction. Therefore, since the time dependence of the power and of the boundary geometry are also retained, the spurious modulation due to the periodic shift of the flux surfaces is automatically taken into account. Modelling with a less accurate equilibrium boundary, derived from EFIT without MSE constraints, no difference is found with respect to Fig. 6. The ion temperature modulation is strongly influenced by the plasma oscillating displacement. The amplitude of the perturbation relative to the average profile is much lower than for the toroidal velocity, as Fig. 2 (c) and (d) show. Moreover, the phase of the high-field side channel of the charge exchange diagnostics is in antiphase with respect to the symmetric channel on the low field side, as plotted in Fig. 1.

CONCLUSIONS

For the first time NBI modulation is used in JET as a tool to investigate toroidal momentum transport combining steady-state momentum balance analysis with the perturbative response of the plasma to a periodic modulation of the torque source. Decoupling the steady-state and the transient effects allows to separate diffusive transport terms from convective ones. The new charge exchange system available on JET measures the toroidal angular velocity with sufficiently high time resolution in order to resolve a single modulation period. In this way, transport analysis can be performed both in steady-state and via Fourier analysis.

The analysis is slightly easier than for NBI based ion heating perturbative studies, because part of the torque is transferred to the plasma immediately via the trapped fast ion orbits. However, the modulation period is not fast enough compared to the beam ions slowing down so that the $\mathbf{J} \times \mathbf{B}$ term is not really dominant according to the reconstruction using TRANSP. Therefore, more careful analysis and eventually predictive modelling are required.

The simple assumption of a constant Prandtl number equal to one is shown to describe the experimental data with sufficient accuracy, provided the Coriolis-like pinch term is included. Of course, the assumption of a constant Prandtl number, in time and space, is not necessarily valid in general, although it is predicted by pure ITG theory. However, the perturbative technique, obtained here with NBI modulation, appears to be a strong constraint for the modelling. The existence of a pinch term, already observed experimentally in the spontaneous rotation discharges in several tokamaks, is necessary for a prediction of the time-dependent angular velocity and it has to be of the size of the Coriolis pinch derived by gyrokinetic theory. The best predictions are obtained for $\text{Pr}_\phi=1.5$, but also $\text{Pr}_\phi=1$ yields acceptable predictions, in particular for the steady-state and amplitude profiles. Without the pinch velocity, the best agreement with the experimental steady-state profile is obtained for $\text{Pr}_\phi=0.5$, but obviously the amplitude and phase profiles are predicted to be much steeper than the measured ones. Therefore, the inclusion of the Coriolis pinch term accounts for a factor 3 between the diffusive transport coefficient as derived from theory and the effective viscosity, the only quantity which can be derived from the experimental transport analysis of steady-state profiles alone.

Some care needs to be taken when addressing the definition of the plasma momentum diffusivity. Depending on the choice of equation 2 or equation 3, the same Prandtl number can lead to different momentum transport levels and therefore different angular velocity predictions, depending on the density peaking. With a typical density profile shape for a JET H-mode discharge, the difference corresponds to roughly 30 % in terms of Prandtl number.

The effect of a modulated plasma displacement is shown to be little, although not completely negligible. The difference between neighbouring charge exchange channels on the high and low field side help quantifying its relative importance.

The perturbative technique proves a valuable tool in order to decouple convective and diffusive transport coefficients for the radial transport of the toroidal angular momentum. The results pre-

sented in this paper show that the simple ITG model of a constant Prandtl number is validated against steady-state and time-dependent profiles from perturbative JET experiments. Our predictive modelling including a Coriolis-like pinch velocity helps reconciling the theoretical finding of ITG theory predicting a Prandtl number close to one and experimental evidence for lower values of the effective viscosity.

ACKNOWLEDGEMENTS

This work, supported by the European Communities under the contract of Association between EURATOM and IPP Garching, was carried out within the framework of the European Fusion Development Agreement. The views and opinions expressed herein do not necessarily reflect those of the European Commission.

REFERENCES

- [1] H. Biglari *et al.*, *Physics of Fluids B* **2** (1990), 1
- [2] R. E. Waltz *et al.*, *Physics of Plasmas* **1** (1994), 2229
- [3] T. S. Hahm, K. H. Burrell, *Physics of Plasmas* **2** (1995), 1648
- [4] E. J. Synakowski *et al.*, *Physical Review Letters* **78** (1997), 2972
- [5] C. M. Greenfield *et al.*, *Physical of Plasmas* **4** (1997), 1596
- [6] H. Shirai *et al.*, *Nuclear Fusion* **39** (1999), 1713
- [7] J. E. Rice *et al.*, *Nuclear Fusion* **47** (2007), 1618
- [8] A. Scarabosio *et al.*, *Plasma Phys. Control. Fusion* **48** (2006), 663
- [9] J. E. Rice *et al.*, *Nuclear Fusion* **39** (1999), 1175
- [10] J. S. deGrassie, *Physics of Plasmas* **11** (2004), 4323
- [11] Y. Sakamoto, *Plasma Phys. Control. Fusion* **48** (2006), A63
- [12] L. G. Ericsson, *Plasma Phys. Control. Fusion* **39** (1997), 27
- [13] G. Tardini *et al.*, *Nuclear Fusion* **42** (2002), 258
- [14] A. G. Peeters *et al.*, *Nuclear Fusion* **42** (2002), 1376
- [15] A. G. Peeters, C. Angioni, *Physics of Plasmas* **12** (2005), 072515
- [16] D. Nishijima *et al.*, *Plasma Phys. Control. Fusion* **47** (2005), 89
- [17] P. de Vries *et al.*, *Plasma Phys. Control. Fusion* **48** (2006), 1693

- [18] A. G. Peeters *et al.*, Physical Review Letters **98** (2007), 265003
- [19] R. J. Goldston, in Basic Physical Processes of Toroidal Fusion Plasmas (Proc. Course and Workshop Varenna, 1985) EUR-10418-EN, (CEC, Brussels, 1986) Vol. 1, p. 165.
- [20] K. D. Zastrow *et al.*, Nuclear Fusion **38** (1998), 257
- [21] M. Kotschnreuther *et al.*, Physics of Plasmas **2** (1995), 2381
- [22] A. Pankin, D. McCune, R. Andre *et al.*, Comp. Phys. Comm. **159**, No. 3
- [23] G. V. Pereverzev, P. N. Yushmanov, IPP report 5/98 (2002)
- [24] L.E.Zakharov and A.Pletzer, Physics of Plasmas **6** (1999), 4693
- [25] J. Weiland, H. Nordman, Proceedings of the 33rd EPS Conference, Rome (2006), ECA Vol. 301, P-2.186
- [26] R. E. Waltz *et al.*, Physics of Plasmas **4** (1997), 2482
- [27] D. Strintzi *et al.*, Physics of Plasmas **15** (2008), 044502

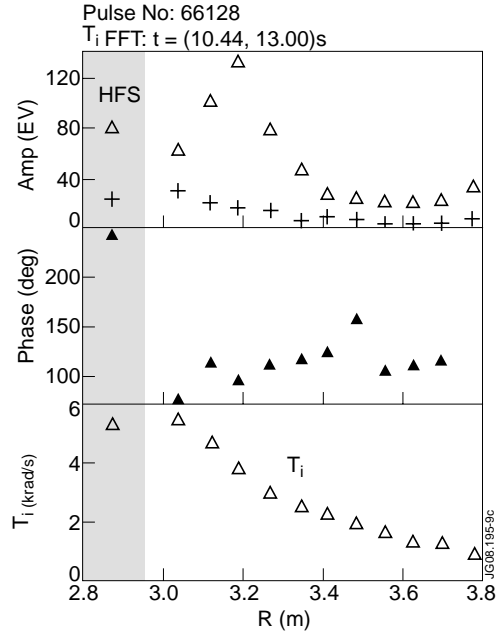


Figure 1: Fourier transform of T_i in the time interval $[10.44, 13.0]$ s. The modulation is less strong than for ω_ϕ and the phase delay higher. The channel on the high field side is perfectly in antiphase.

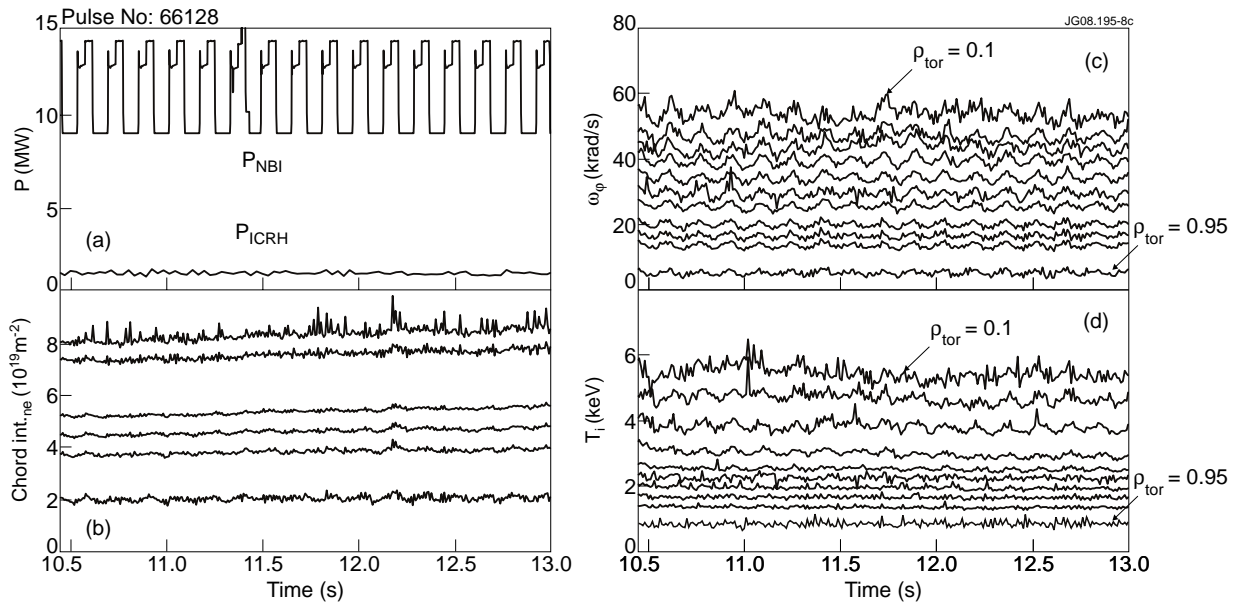


Figure 2: Time traces in the time interval selected for the analysis. Heating power (a), chord integrated density from interferometer (b), charge exchange measurements of ω_ϕ (c) and T_i (d). The effect of the modulation is strongest for ω_ϕ (3-6%), moderate for T_i (1-2%) and negligible for n_e .

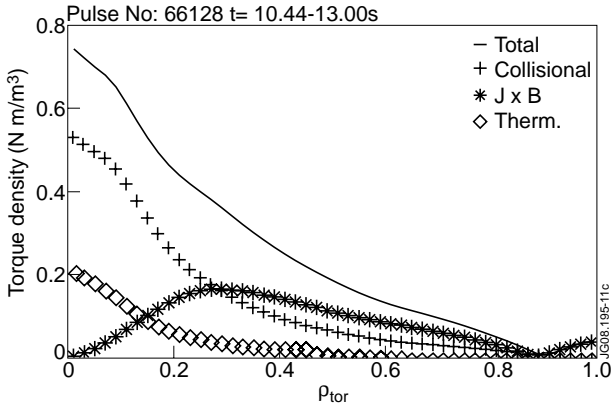


Figure 3: Time averaged torque density profiles from TRANSP calculations. Total (continuous line), collisional (crosses), $J \times B$ (stars) and thermalisation (diamonds).

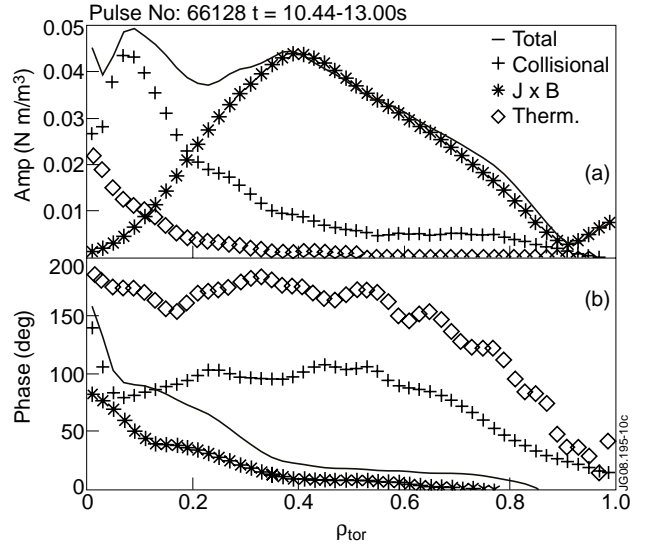


Figure 4: Fourier transformed torque density perturbation profile at the fundamental frequency from TRANSP. (a) Amplitude and (b) phase. Symbols as in Fig.3.

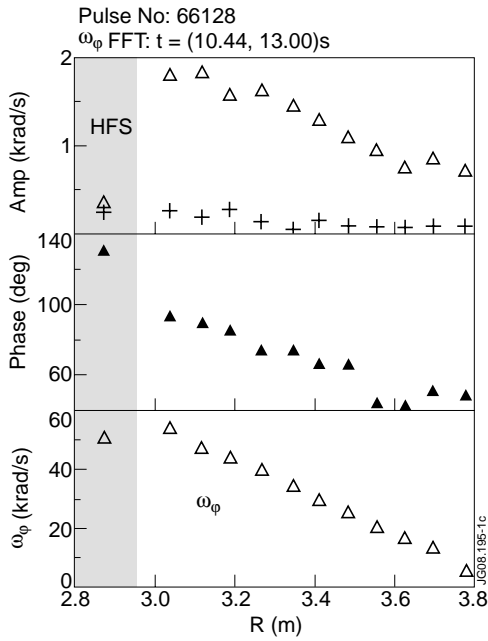


Figure 5: Fourier transform of the experimental angular velocity. The shaded region corresponds to the high field side of JET. The crosses are a measure of the noise level.

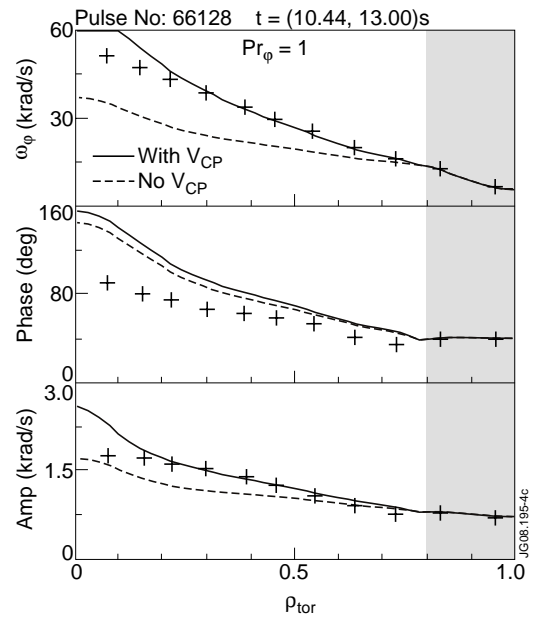


Figure 6: Prediction of the toroidal angular velocity profile assuming $Pr_\phi = 1$. With the simplified formula for the Coriolis pinch (continuous line) and setting it to zero (dashed line). Outside $\rho_{tor} = 0.8$ (shaded region) no transport equation is solved. The crosses are the experimental data.

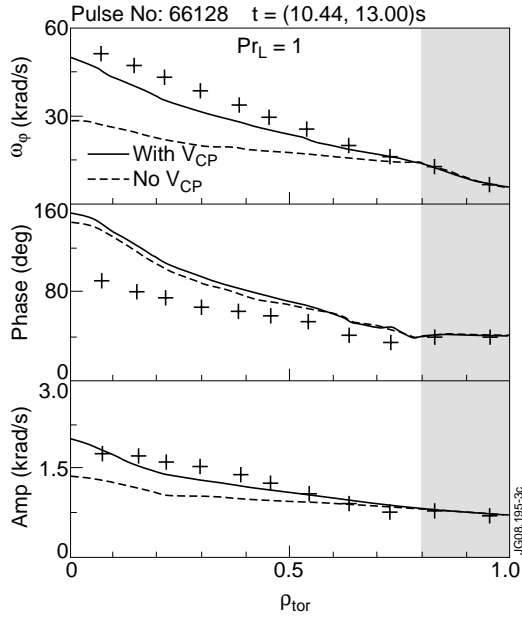


Figure 7: Modelling of the toroidal angular momentum assuming $Pr_L = 1$.

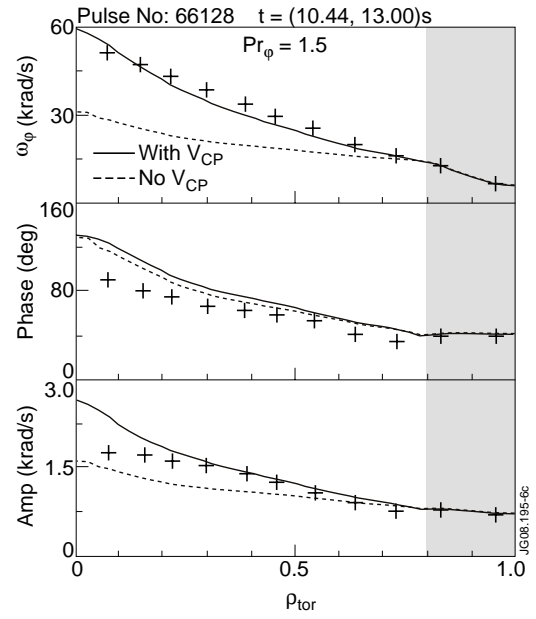


Figure 8: Prediction of the toroidal angular velocity profile assuming Prandtl number equal to 1.5. Lines like in Fig.6.

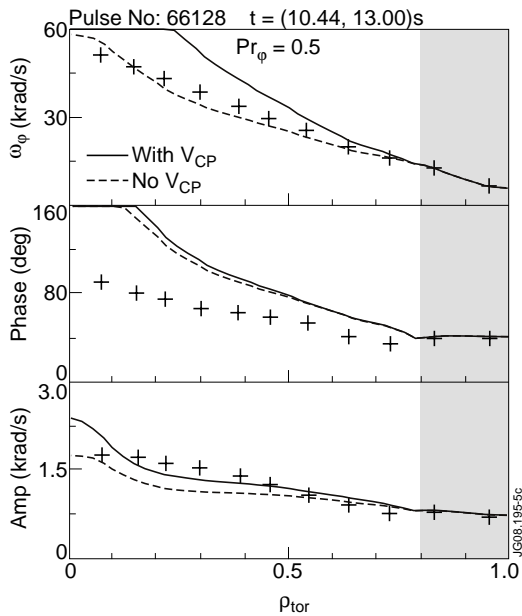


Figure 9: Prediction of the toroidal angular velocity profile assuming Prandtl number equal to 0.5. Lines like in Fig.6.

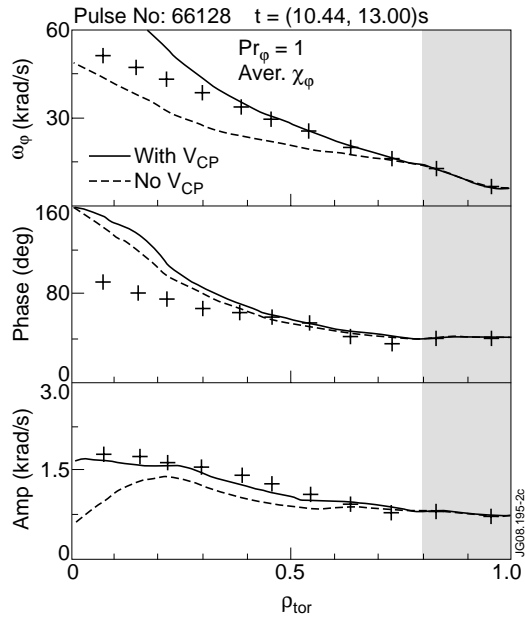


Figure 10: Modelling of the toroidal angular momentum assuming constant χ_ϕ taken as the time averaged χ_i profile in the interval 10.44-13.0s.

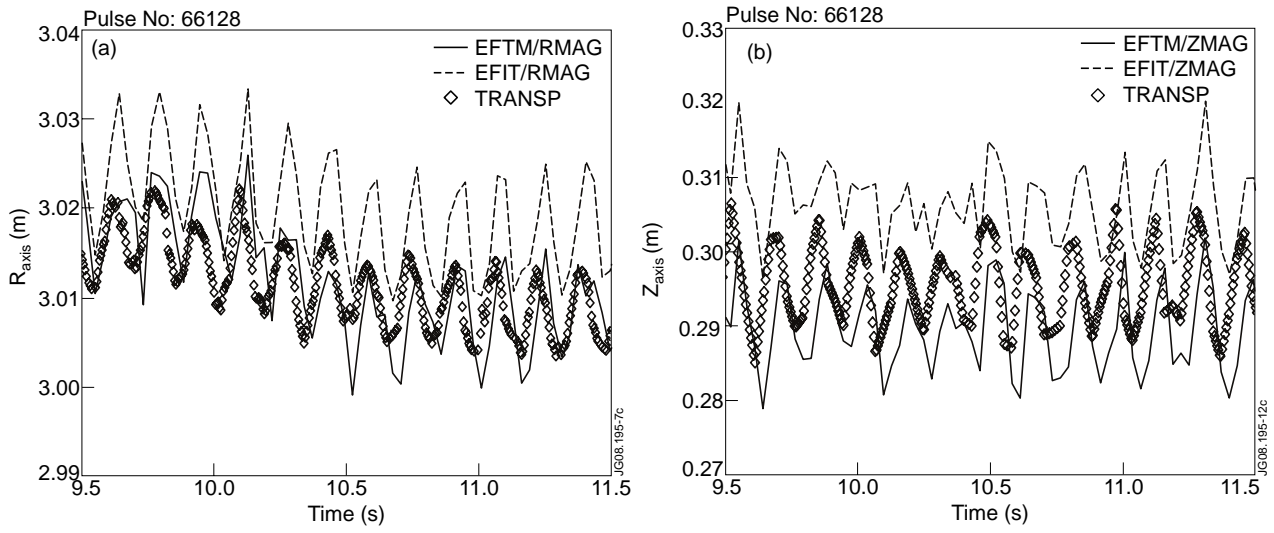


Figure 11: Oscillation of R_{mag} (a) and of z_{mag} (b) of the magnetic axis in time due to the NBI modulation. Equilibrium with MSE data constraint (continuous line) and without (dashed line).